Damping of friction-induced vibrations applying parallel compensator

Golovin I., Palis S., Timoschenko A., Klepikov V.
ievgen.golovin@ovgu.de

Abstract

In this contribution a new damping approach of friction-induced self-excited vibrations is presented. The idea is to extent the conventional drive control system with an additional parallel compensator. For this purpose a mathematical model of a generic two degree-of-freedom electromechanical system with a nonlinear friction curve and a classical cascade drive control is investigated. It has been shown that the classical cascade approach can not solve the problem of self-excited vibrations without an additional sensors or redesign of feedback control law. However, utilizing the parallel compensation as an extension for conventional control scheme gives promising results.

1 Introduction

In many electromechanical systems a number of different frictional effects has to be taken into account. In some cases, when the friction curve has a negative slope [1, 2], self-excited oscillations may occur [3, 4, 5]. In most cases these oscillations decrease the operational performance and can lead to mechanical breakdowns. Their occurrence has been reported in different areas, e.g. rail transport, metal-working machinery, bridge cranes, rolling mills, industrial robots, drilling systems etc. [3, 6, 7]. In order to solve the described problem several approaches have been proposed [6, 8, 9]. All of them are based on designing a complex control law. However the majority of electric drive systems are equipped with power converters which have their own software and conventional drive control system. Implementing a new control law in this case becomes difficult and thus increases costs considerably.
In this contribution a different approach will be presented allowing the application of standard drive control systems. The closed loop stability can be preserved applying an additional compensator acting in parallel with the drive control system. For this purpose, a generic two degree-of-freedom electromechanical system with a nonlinear friction curve and conventional cascade drive control is studied. The parallel compensator augmenting the conventional feedback control system is derived by straightforward root locus design.
The contribution is structured as follows: in section 2 the mathematical model of a generic electromechanical two degree-of-freedom (DoF) system with nonlinear friction curve is introduced and analyzed. In section 3 the main problems applying

standard control approaches are presented. In section 4 the design procedure for an appropriate parallel compensator is proposed.

2 Mathematical modelling and stability

As a simple simulation model a prototypic electromechanical system with two DoF and nonlinear friction curve is studied (Fig. 1). Here, the first mass is actuated by the DC motor with separately excited field winding whereas friction loads are acting on the second mass. The equations of motion can be represented as follows:

$$J_1 \frac{d\omega_1(t)}{dt} = \tau_1(t) - \tau_y(t), \tag{1}$$

$$\tau_y(t) = c_{12} \int_0^t (\omega_1(\tau) - \omega_2(\tau))d\tau + b_{12}(\omega_1(t) - \omega_2(t)), \tag{2}$$

$$J_2 \frac{d\omega_2(t)}{dt} = \tau_y(t) - \omega_2(t)\tau_f(\omega_2), \tag{3}$$

where J_1 and J_2 are inertial masses of the drive system and the actuator, $\omega_1(t)$ and $\omega_2(t)$ are angular velocities of two masses, c_{12} and b_{12} are torsional stiffness and damping of linear spring connection between masses, $\tau_1(t)$ is the drive torque, $\tau_y(t)$ is the elastic torque and $\tau_f(\omega_2)$ is the friction load torque function depending on the second mass angular velocity.

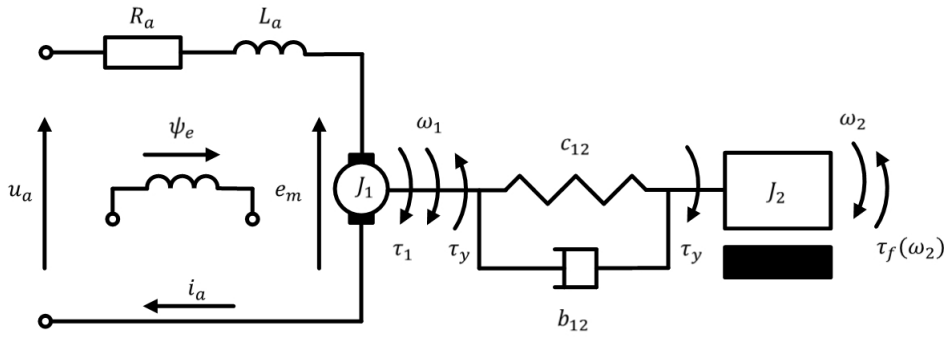

Figure 1: Two DoF electromechanical system with nonlinear friction load

The governing equation of DC motor armature circuit can be derived based on Kirchhoff's voltage law:

$$u_a(t) = e_m(t) + R_a i_a(t) + L_a \frac{di_a(t)}{dt}, \tag{4}$$

where $u_a(t)$ and $i_a(t)$ are armature voltage and current, R_a and L_a are armature resistance and inductance and $e_m(t)$ is electromotive force.
Assuming that the magnetic field is fixed, electrical and mechanical system variables

can be coupled as:

$$\omega_1(t) = \frac{1}{k_m \psi_e} e_m(t), \tag{5}$$

$$\omega_0(t) = \frac{1}{k_m \psi_e} u_a(t), \tag{6}$$

$$\tau_1(t) = k_m \psi_e i_a(t), \tag{7}$$

where k_m is DC motor ratio, ψ_e is constant magnetic field flow and $\omega_0(t)$ is non-loaded angular velocity.
As in equations 1, 2, 3 the motor torque $\tau_1(t)$ is defined as acting variable, a relation between the motor velocity and the motor torque should be derived. Taking into account relations 5, 6, 7 the equation 4 can be reformulated as:

$$\tau_1(t) = \beta\omega_0(t) - \beta\omega_1(t) - T_e \frac{d\tau_1(t)}{dt}, \tag{8}$$

where $\beta = (k_m\psi_e)^2/R_a$ is the slope of the motor mechanical curve and $T_e = L_a/R_a$ is the electromagnetic time constant of the armature circuit.
Modeling of friction loads for a specific system is typically a non-trivial task, due to the limited understanding of the friction phenomenon at hand. This often results in high uncertainties and time variance of model quality. However, for this study the presence of a negative slope region in the friction curve is sufficient to result in the occurrence of instabilities and limit cycles. That is why for a qualitative analysis a simple piecewise linear approximation of a humped friction model with the Stribeck effect can be used (Fig. 2) [3, 9]. Nominal numerical values for this piecewise approximation are given in equation 9. This kind of approximation allows to divide the curve into specific regions and to deal with the linear system in certain region preserving a nonlinear behavior globally. For each curve region the slope parameter for linear model can be expressed as $b_{sn} = \Delta\tau_f/\Delta\omega_s$.

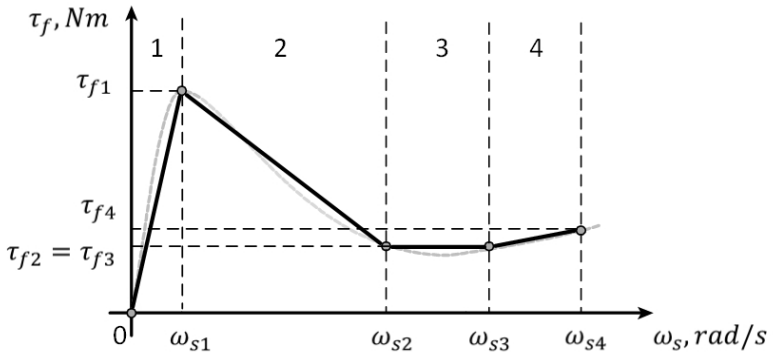

Figure 2: Friction curve

$$\tau_f(\omega_s) = \begin{cases} 50\omega_s\ , & 0 < \omega_s < 5\ rad/s \\ -1.2\omega_s + 255\ , & 5 < \omega_s < 155\ rad/s \\ 100\ , & 155 < \omega_s < 165\ rad/s \\ 1.43\omega_s - 135.7\ , & 165 < \omega_s < 200\ rad/s \end{cases} \tag{9}$$

Applying the Laplace transformation, the above modeling equations 1, 2, 3 and 8 can be represented for a certain region of operating points in terms of the Laplace variable s.

$$\omega_1(s) = \frac{1}{J_1 s}(\tau_1(s) - \tau_y(s)), \tag{10}$$

$$\tau_y(s) = \frac{c_{12}}{s}(\omega_1(s) - \omega_2(s)) + b_{12}(\omega_1(s) - \omega_2(s)), \tag{11}$$

$$\omega_2(s) = \frac{1}{J_2 s}(\tau_y(s) - \omega_2(s) b_{sn}), \tag{12}$$

$$\tau_1(s) = \frac{\beta}{T_e s + 1}(\omega_0(s) - \omega_1(s)). \tag{13}$$

The equivalent block diagram is illustrated in Fig. 3.
As has been mentioned above, the source of instability in the model is, from a mathematical point of view, the occurrence of the negative slope ratio b_{sn} for specific regions of the friction velocity curve. For the linear piecewise curve (Fig. 2) the unstable dynamics can occur for the region of operating points between angular velocities ω_{s1} and ω_{s2}. This phenomenon, i.e. the decrease of the friction torque for an increased velocity, results in a further acceleration assuming a constant motor torque. In practical applications negative slope of the friction curve occurs only in a limited region and would therefore prevent the system from speeding up infinitely. Nevertheless, this mechanism of instability may result in limit cycles, i.e. nonlinear oscillations with high amplitudes, which is a frequently observed phenomenon leading to decreased system performance and damages.

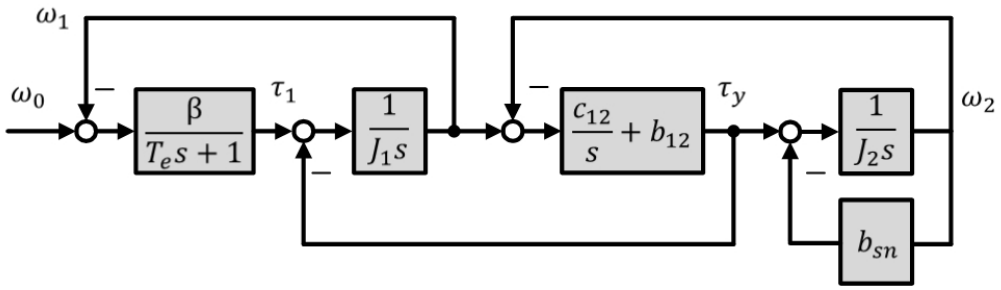

Figure 3: Block diagram of two DoF's electromechanical system

In order to analyze the stability properties of linearized system (Fig. 3), poles location of the transfer function $G(s) = \omega_2(s)/\omega_0(s)$ for a set of nominal parameter values (Tab. 6) and for varying uncertain slope ratio $-1 < b_{sn} < 0.1$ has been obtained. As can be seen from Fig. 4, the transfer function has one real and one complex pole pair. It should be also stressed, that the fast pole at $s = -10$ is not depicted in figure and its location does not depend on the ratio b_{sn}. From Fig. 4 it also becomes apparent that for small negative friction coefficients, i.e. $b_{sn} <$ - 0.1, the complex pole pair moves into the right-half plane (RHP) which results in an unstable system dynamics. It should be emphasized that this instability is a local effect for the described linear system resulting globally in nonlinear oscillations.

T_e	0.1	$[s]$
β	0.5	$[(V/(rad\ s))^2/\Omega]$
J_1	3	$[kg\ m^2]$
J_2	2	$[kg\ m^2]$
c_{12}	100	$[Nm/rad]$
b_{12}	0	$[Nm\ s/rad]$
ω_0	100	$[rad/s]$

Table 6: System model parameters

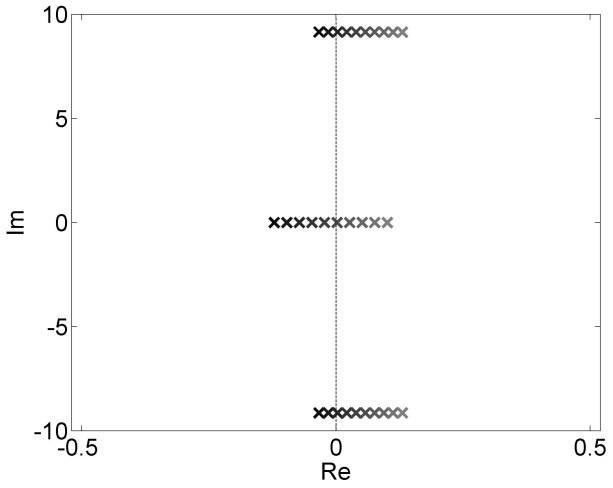

Figure 4: Root locus for slope variations ($b_{sn} = 0.1$ (black) and $b_{sn} = -1$ (gray))

3 Problem of standard control approaches and zero dynamics

3.1 Conventional electric drive control system

In the modern machines and mechanisms design controlled electric drives have become a quasi-standard. In order to control the electric energy flow, these drive systems are equipped with power converters based on thyristor or transistor schemes. In most cases manufacturers provide a complex product augmenting their converters by a fully-parameterizable standard control system and a manufacture-specific software solution. Although, such a design allows fast engineering solutions in many application cases, whereas implementation of non-standard control laws by the user is at least difficult if not impossible.
Velocity control of the electric drive is one of the classical tasks for different electromechanical systems. In this case the cascade control with PI controllers is the most widely used control structure (Fig. 5). It includes an inner current (or sometimes torque) control loop $G_i(s)$ and an outer velocity control loop $G_\omega(s)$. The inner controller $C_{i,PI}(s)$ for the motor current plant $P_i(s)$ is designed first, after which the outer controller $C_{\omega,PI}(s)$ for the whole plant $G_i(s)$ and $P_\omega(s)$ is designed.

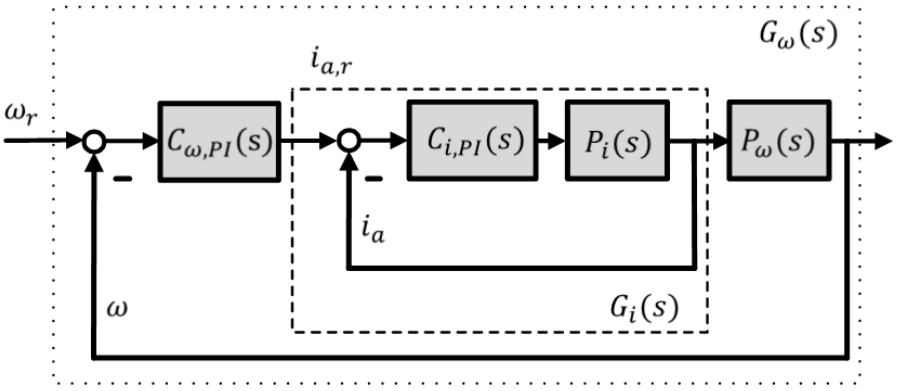

Figure 5: Standard cascade control

The electrical subsystem $P_i(s)$ is classically represented by two first order systems, the rectifier associated with the time constant T_μ and the electrical part of the motor (eq. 13) with the time constant T_e, where $T_\mu \ll T_e$. As the motor torque $\tau_1(t)$ has been defined as acting variable, the open loop plant $P_i(s)$ should also consider relations 6 and 7. For the current controller a standard PI control structure is chosen.

$$P_i(s) = \frac{i_a(s)}{u_c(s)} = \frac{1}{T_\mu s + 1}\frac{\beta}{T_e s + 1}\frac{1}{(k_m\psi_e)^2}, \tag{14}$$

$$C_{i,PI}(s) = \frac{u_c(s)}{e_i(s)} = k_i\frac{T_i s + 1}{T_i s}. \tag{15}$$

Here, $u_c(s)$ is the controller voltage, $e_i(s)$ is the measured inner loop error, k_i and T_i are the PI-controller parameters.
Applying the modulus (magnitude) optimum tuning procedure [10] as a standard controller design procedure for electric drive systems PI-controller parameters are given by $k_i = T_e(k_m\psi_e)^2/(2T_\mu\beta)$ and $T_i = T_e$. Here, the main idea is to compensate the largest time constant T_e in order to achieve fast reference tracking.
In a second step the outer controller is designed for the closed inner loop $G_i(s)$ and the mechanical motor subsystem $P_\omega(s) = (k_m\psi_e)/(J_1 s)$. In order to achieve both good reference tracking and disturbance rejection the parameters of the velocity PI-controller can be adjusted according to the symmetrical optimum so that $k_\omega = J_1/(4T_\mu k_m\psi_e)$ and $T_\omega = 8T_\mu$.

$$C_{\omega,PI}(s) = \frac{i_{a,r}(s)}{e_\omega(s)} = k_\omega\frac{T_\omega s + 1}{T_\omega s} \tag{16}$$

Using these tunings for both loops with a reference prefilter $G_r(s) = 1/(8T_\mu s + 1)$ gives an overshoot of approximately 8% and a settling time of approximately 26 T_μ [10, 11].

$k_m\psi_e$	1	[-]
T_μ	0.01	$[s]$
k_i	10	[-]
T_i	0.1	$[s]$
k_v	75	[-]
T_v	0.08	$[s]$
T_r	0.08	$[s]$

Table 7: Control system parameters

3.2 Problem of unstable zero dynamics

The above described conventional control scheme and tuning procedures are widely used by engineering companies in practice. The velocity measurements in electromechanical systems are often provided with incremental or optical sensors on the motor shaft. A direct velocity measurements on the working element of the mechanisms increase costs and are often complicated or even impossible. From the theoretical point of view this means that the first mass velocity can be measured for electromechanical systems with more than one DoF only.
In order to investigate the behavior of the cascade control scheme for the two DoF electromechanical system with friction, the transfer function for the overall system, i.e. including the inner current loop $G_i(s)$, the two DoF system with frictional load and the inner counter electromotive force feedback, has to be obtained. Taking into account the models from Fig. 3 and Fig. 5, the open loop velocity transfer function can be expressed as:

$$P_{\omega,m}(s) = \frac{\omega_1(s)}{i_{a,r}(s)} = \frac{k_i\beta(T_e s + 1)(J_2 s^2 + b_{sn} s + c_{12})}{Q(s)}, \tag{17}$$

where $Q(s)$ is the polynomial of the open loop plant denominator.
In order to study the overall dynamic behavior the above presented velocity controller $C_{\omega,PI}(s)$ with the prefilter $G_r(s)$ is applied to the transfer function 17. Taking into account model parameters from Tab. 6, Tab. 7 and the nominal value of slope coefficient $b_{sn} = -1.2$ for a falling region of curve (eq. 9) the resulting pole-zero plot is depicted in Fig. 6. As can be seen the closed loop system has two RHP poles and is hence unstable. It should be stressed that this problem exists due to the presence of RHP zeros in the numerator term $J_2 s^2 + b_{sn} s + c_{12}$ of the equation 17 which occur for slope ratio $b_{sn} < 0$. Systems with unstable zero dynamics, i.e. possessing RHP zeros, are challenging from a control point of view as they are well-known to be unstable under high controller gains and the locations of system zeros are invariant with respect to feedback.
A conventional solution approach would involve a full controller redesign increasing the overall control system complexity significantly. However, as has been mentioned above implementation of new control structures in electric drive system is in most cases expensive and time-consuming. In this contribution a different approach will be presented allowing the application of a standard drive control system augmented by an additional parallel compensator as illustrated in Fig. 7. Here, the first step

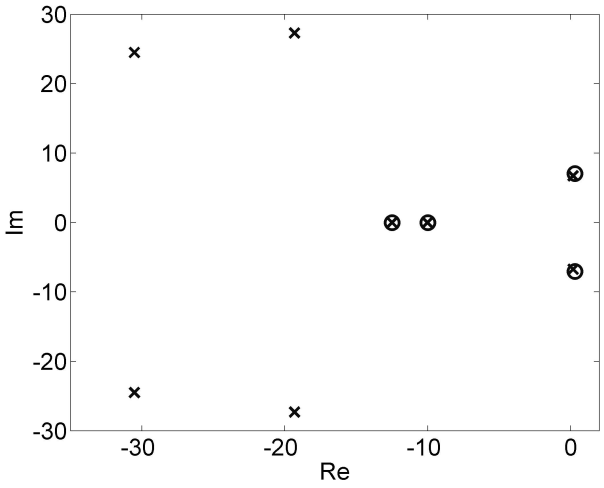

Figure 6: Pole-zero plot of the closed loop system applying a conventional velocity control

is to design an appropriate parallel compensator stabilizing the friction-induced unstable zero dynamics. Secondly, the standard feedback controller may be retuned in order to stabilize RHP poles.

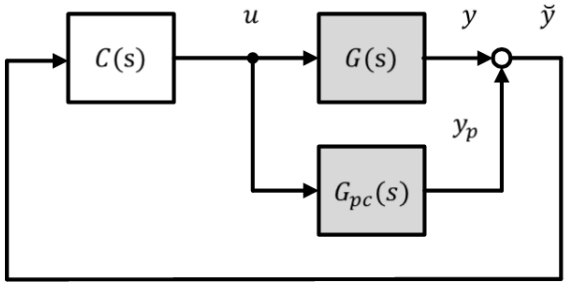

Figure 7: Overall control structure

4 Parallel compensator design

In order to influence the stability behavior of the zero dynamics an appropriate parallel compensator as depicted in Fig. 8 has to be designed [12].
In case of a single-input single-output system the associated transfer function $G(s)$ can be separated into four fractions

$$G(s) = \frac{N^+(s)N^-(s)}{D^+(s)D^-(s)}, \tag{18}$$

where $N^+(s)$ and $D^+(s)$ contain the left-half plane (LHP) zeros and poles and $N^-(s)$ and $D^-(s)$ the RHP zeros and poles. It is assumed that the parallel compensator

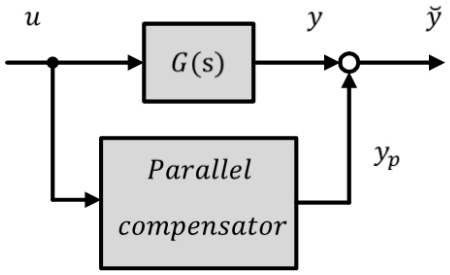

Figure 8: Parallel compensator

consists of the fractions containing all plant poles and zeros in the left half plane, i.e. $N^+(s)$ and $D^+(s)$, plus two additional fractions $N_c(s)$ and $D_c(s)$.

$$G_{pc}(s) = \frac{N^+(s)N_c(s)}{D^+(s)D_c(s)}. \tag{19}$$

The parallel connection of the plant $G(s)$ and the parallel compensator $G_{pc}(s)$ results in

$$G_s(s) = G(s) + G_{pc}(s) = \frac{N^+(s)\left[N^-(s)D_c(s) + N_c(s)D^-(s)\right]}{D^+(s)D^-(s)D_c(s)}. \tag{20}$$

It can be shown that the design of a parallel compensator stabilizing the unstable zero dynamics is equivalent to designing a controller $G_c = N_c(s)/D_c(s)$ which stabilizes the virtual plant $G_{vir}(s) = D^-(s)/N^-(s)$.
Taking into account the aforementioned nominal parameters the plant transfer function (17) can be calculated as:

$$G(s) = \frac{1666.7(s^2 - 0.6s + 50)}{(s - 0.24)(s^2 - 0.35s + 83.19)(s^2 + 99.96s + 4998)}. \tag{21}$$

Here, the system can be separated into the following stable and unstable fractions

$$N^-(s) = s^2 - 0.6s + 50, \tag{22}$$
$$D^-(s) = (s - 0.24)(s^2 - 0.35s + 83.19), \tag{23}$$
$$N^+(s) = 1666.7, \tag{24}$$
$$D^+(s) = (s^2 + 99.96s + 4998). \tag{25}$$

In order to achieve stable zero dynamics the following polynomial should have no RHP zeros:

$$1 + G_c(s)G_{vir}(s) = 1 + G_c(s)\frac{(s - 0.24)(s^2 - 0.35s + 83.19)}{s^2 - 0.6s + 50}. \tag{26}$$

Applying the root locus feedback design procedure for the virtual plant G_{vir} an appropriate controller as a simple gain $G_c = 0.11$ can be designed which results in the following parallel compensator considering equation 19

$$G_{pc}(s) = \frac{183.34}{(s^2 + 99.96s + 4998)}. \tag{27}$$

Applying the designed compensator hence yields a new system with locally stable zero dynamics. In this specific example no additional controller retuning is needed and hence the above presented PI-controller can be used. Simulation results with and without the designed parallel compensator are depicted in Fig. 9 (right) and (left), respectively. As can be seen in Fig. 9 (left), assuming piecewise linear approximation of friction curve (eq. 9) the aforementioned unstable zero dynamics leads to system instability and the occurrence of nonlinear oscillations.

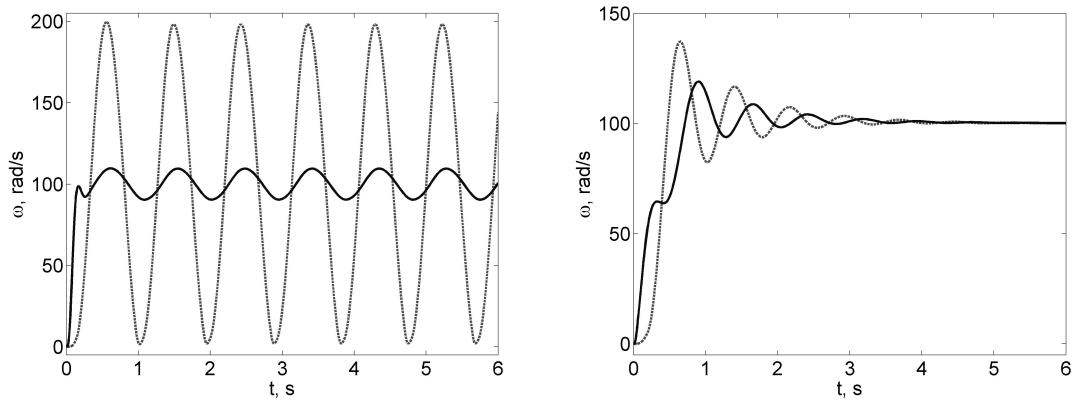

Figure 9: Angular velocities of the first (solid black) and second (dotted gray) masses without (left) and with (right) parallel compensator

Conclusion and future work

A new damping approach of friction-induced self-excited vibrations has been proposed. The mathematical model of two degree-of-freedom electromechanical system with the nonlinear friction curve and the classical cascade velocity PI-control for electric drive system has been investigated. It has been shown that conventional control approaches may result in the occurrence of self-excited vibrations requiring a controller redesign and often a time-consuming reimplementation. In order to overcome this problem the design of a parallel compensator stabilizing the unstable zero dynamics has been proposed in this contribution.
As has been mentioned, exact friction behavior is often unknown or time-varying. Hence, application of robust or adaptive methods for compensator design is an interesting field for future research.

References

[1] K. Farhang, A. L. Lim, A Non-Phenomenological Account of Friction/Vibration Interaction in Rotary Systems, Journal of Tribology Vol. 128, 2006, pp. 103 - 112.

[2] M. Rahmani, S. Krall, F. Bleicher, Experimental Investigations on Stick-Slip Phenomenon and Friction Characteristics of Linear Guides, Procedia Engineering 100, 2015, pp. 1023 - 1031.

[3] V. Klepikov, Dynamics of Electromechanical Systems with Nonlinear Friction, NTU "KhPI", 2014.

[4] A. Fidlin, Nonlinear Oscillations in Mechanical Engineering, Springer-Verlag Berlin Heidelberg, 2006.

[5] D. P. Hess, Interaction of vibration and friction at dry sliding contacts, Dynamics with Friction: Modeling, Analysis and Experiment, 2001, pp. 1 - 27.

[6] Y.F. Wang, D.H. Wang, T.Y. Chai, Active control of friction self-excited vibration using neuro-fuzzy and data mining techniques, Expert Systems with Applications 40, 2013, pp. 975 - 983.

[7] M.A. Kiseleva, N.V. Kondratyeva, N.V. Kuznetsov, G.A. Leonov, Hidden oscillations in drilling systems with salient pole synchronous motor, IFAC-Papers, 2015, pp. 700 - 705

[8] M. B. Saldivar Marquez, I. Boussaada, H. Mounier, S. I. Niculescu, Analysis and control of oilwell drilling vibrations: a time-delay systems approach, Springer, 2015.

[9] N. MihajloviДЉ, Torsional and Lateral Vibrations in Flexible Rotor Systems with Friction, Technische Universiteit Eindhoven, 2005.

[10] C. Bajracharya, M. Molinas, J. A. Suul, T. M. Undeland, Understanding of tuning techniques of converter controllers for VSC-HVDC, Nordic Workshop on Power and Industrial Electronics, 2008.

[11] D. Schröder, Elektrische Antriebe - Grundlagen, Springer, 2013.

[12] S. Palis, A. Kienle, Discrepancy based control of particulate processes, Journal of Process Control 24, 2014, pp. 33 - 45.

Ievgen Golovin, Otto-von-Guericke University Magdeburg, Universitätsplatz 2, 39106 Magdeburg, Germany
Stefan Palis, Otto-von-Guericke University Magdeburg, Universitätsplatz 2, 39106 Magdeburg, Germany
Andrii Timoschenko, NTU "Kharkiv Polytechnic Institute", Frunse 21, 61002 Charkov, Ukraine
Vladimir Klepikov, NTU "Kharkiv Polytechnic Institute", Frunse 21, 61002 Charkov, Ukraine